

# UC Irvine

## UC Irvine Previously Published Works

### Title

Thermal, ablative, and physicochemical effects of XeCl laser on dentin

### Permalink

<https://escholarship.org/uc/item/4nx4870z>

### ISBN

9780819417411

### Authors

Lee, Jon P  
Cheung, Eric M  
Wilder-Smith, Petra BB  
[et al.](#)

### Publication Date

1995-05-01

### DOI

10.1117/12.207441

### Copyright Information

This work is made available under the terms of a Creative Commons Attribution License, available at <https://creativecommons.org/licenses/by/4.0/>

Peer reviewed

# Thermal, Ablative, and Physicochemical Effects of XeCl Laser on Dentin

Jon P. Lee, Eric Cheung, Petra Wilder-Smith,  
T.J. Desai, L.H. Liaw, M.W. Berns and Joseph Neev

Beckman Laser Institute and Medical Institute, University of California, Irvine  
1002 Health Sciences Road East, Irvine, CA 92715, (714) 856 6996 FAX 856-8413

## Key Words:

Microhardness, XeCl excimer, dentin, thermal camera, ablation rate, scanning electron microscopy, physicochemical

## Abstract

Previous studies have reported altered dentinal structure and properties after laser irradiation. It was the aim of this investigation to determine the thermal and ablative effects of XeCl irradiation in dentin and then to investigate microstructural and physicochemical changes in the residual dentin structure. Extracted human molar tooth roots were bisected and coated with acid-resistant varnish, leaving a window. After irradiation of one half at 1 Hz, 15 ns pulse durations, fluences of  $0.5\text{-}2\text{J}/\text{cm}^2$ , both halves were subjected to acidified gelatin gel at pH 4.5. The carious lesions were bisected and used to perform SEM and microhardness measurements.

## 1. Introduction

Lasers were first applied to dental tissue in 1964 (1) and were soon followed by a large body of research. Results demonstrated that laser interaction with enamel and dentin is possible but not without extensive thermal and mechanical damage. Such adverse effect prevented the quick development of an accepted practical device. Among the various lasers which were studied were CW CO<sub>2</sub>, Nd:YAG, Argon ion and dye lasers as well as pulsed systems (CO<sub>2</sub>, Nd:YAG, Ho:YAG and Er:YAG, ArF and XeCl excimer lasers, and pulsed CO<sub>2</sub>). (2-10). Development of a laser drill - a device that would painlessly and efficiently remove hard dental tissue with high accuracy and with a potentially high degree of precision, still needs to be accomplished. Additional applications of lasers include surface modification, root canal preparations and caries removal and sterilization of teeth, among others.

A potentially useful laser class for applications such as surface modification and tissue preparation, is the pulsed XeCl excimer laser. In spite of its low ablation rate, this laser is characterized by minimal thermal effects and lower penetration depths that yield highly controlled, highly precise surface features (11, 12, 13). These characteristics are especially desirable to applications in restorative dentistry. Over the past few years we have investigated various features of this laser class such as ablation plume dynamics, thermal effects and damage, ablation rates, plasma emission characteristics, and surface morphology (3, 4, 10, 13).

Traditional measures for caries-prevention provide a protective effect of approximately 50%. Methods available to us include dietary measures, fluorides, and a wide range of varnishes and sealers. (14, 15, 16). Disadvantages of these traditional methods include a need for continual patient motivation with regard to dietary and oral hygiene measures, and apprehensions about the possible side effects of excess fluoride. A further disadvantage of fluoride applications is the finding that not all surfaces of the tooth are afforded equal protection by these measures. (14)

The purpose of this investigation is to examine and correlate the ablation characteristics of the pulsed XeCl laser to their effects on root dentin microstructure and microhardness. IR thermography, scanning electron microscopy (SEM), and microhardness measurements were used synchronously so that a more complete picture of the interaction and its effects can be obtained.

## 2. Materials and Methods

The study employed sixteen human maxillary and mandibular molar teeth fixed in 10% thymol. Prior to their preparation, the soft tissue and debris were removed by using a rotary wire abrasive brush followed by rinsing in 2.5% NaOCl for 30 minutes. Initial sectioning of the teeth was accomplished by cutting horizontally at each tooth using a microstructural rotary saw with a diamond coated edge (Isomet, Buehler Ltd., Lake Bluff, IL, USA). One transversal cut was made near the cemento-enamel junction to separate the crown and other apical areas of the tooth to minimize the amount of enamel on the specimens. Afterward, the saw cut each of the remaining molar tooth sections into thinner slices varying from 0.3 mm<sup>2</sup> to 1.0 mm<sup>2</sup>. The tooth roots which remained on the saw block were saved for later studies (see below) while the thin slices were stored in 10% thymol to be used in ablation rate (AR) and thermal perturbation studies.

Two different methods were employed for the determination of AR, depending on the thickness of the dentin slices. Dentin slices were ablated with the output energy at 5mJ, 25mJ, and 70 mJ per pulse and pulse repetition rate at 2Hz. Ablation rate studies using the penetration method were performed on the thinnest slices of dentin, using a HeNe laser to determine the end point. In the penetration method, the thickness of the slice is known while the time taken to penetrate the slice is the measurable variable. Alternatively, the depth of the ablation crater was measured using an interferometric objective on a calibrated light microscope (Labophot-2, Nikon, Tokyo, Japan). This method allowed the experimenter to measure the actual depth of the crater from lip to bottom after the impact of a known number of pulses. By moving the calibrated fine focus, the interference pattern can be observed to converge to the center of the crater's bottom or diverge towards the crater's surface. Both methods yielded roughly the same quantitative results which were then averaged. The specimens were removed from their storage vials and immediately mounted for ablation without allowing the air to dry them. This procedure kept the specimens fresh and moist with regard to water-content during irradiation since recent studies on enamel have shown water-content to be a factor in ablation efficiency (17). Furthermore, it allowed the experiment to be performed on dentin slices that more closely resembles the teeth within the humid conditions of the mouth.

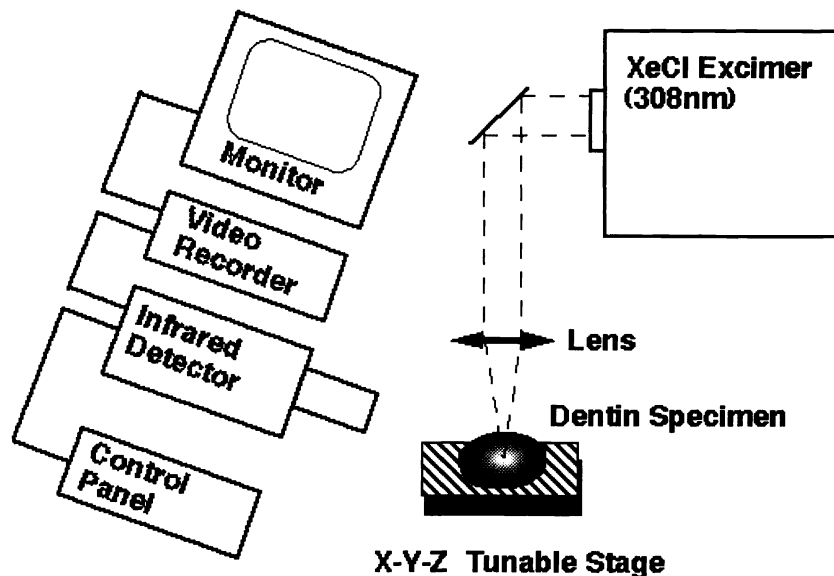


Figure 1: Typical set up for the measurement of thermal characteristics on the dentin surface. The dentin specimens were mounted on an x-y-z stage. The laser beam was focused on to the bone specimen by a convex lens with a focal length of 10 cm.

The thermal camera, specimens, and laser were configured as schematically illustrated in Figure 1. The thermal camera (Model 600, Inframetrics, North Bellerica, MA, USA) allowed us to measure the effects

of the ablating pulse repetition rate (PRR) and fluence on the surface temperature. The camera uses oscillating mirrors to scan the field of view horizontally and vertically and produce images at a rate of 30 frames per second. The camera employs a mercury-cadmium-tellurium detector which is sensitive at the 8 - 12 $\mu$ m range. The detector's specified response time is 1 $\mu$ s, with a sampling rate of 2.01MHz. The manufacturer's specified minimum detectable temperature difference is 0.1 °C with temperature ranges varying from 5 °C to 2000 °C. As real time images are captured on video, the sampling time of this system is one image every 33 ms. The images were recorded using a professional quality VCR and subsequently analyzed.

Since the camera's detector was not synchronized with the laser, and since each pixel point in our thermal camera is updated every 1/30th of a second, transient thermal effects on the time scale of the ablation pulse (15ns) or even slower events, on time scales shorter than 30 millisecond (ms) are not resolved, in spite of the detector's relatively fast response time. The camera data, thus, represent the tissue's slow, time-dependent thermal response and the cumulative effects of consecutive pulses.

In each ablation site, temperature measurements using the point mode of the thermal camera were made. In this manner thermal characteristics of the laser treated surface could be quantified. Specifically, the hottest temperature at the center of the thermal disturbance was recorded for each individual laser pulse. Thermal studies were conducted with energies of 20 and 40 mJ and PRR of 1, 5, and 9 Hz.

The remaining molar tooth roots (from the original sectioning) were bisected to expose a smooth surface of dentin. The exposed surfaces were coated with an acid-resistant varnish. A 9 x 9 mm window of unvarnished dentin was preserved leaving a surface for acid treatment. These halves were stored in 10% thymol at 25° C until time of irradiation. The hemi-sectioned tooth roots were irradiated at 1 or 10 Hz with 15ns pulses and fluences of 0.08 J/cm<sup>2</sup> and 2.4 J/cm<sup>2</sup> (Figure 2). These laser treated specimens and the control group (which was not laser treated) were then subjected to artificial caries formation using 10% acidified gelatin gel at pH 4.5. The artificial caries created by this process were identified using a low-power light microscope. The caries sites were then bisected and examined by SEM. The hardness of the tooth in both groups was evaluated at the tooth surface using a 25g indenter on a microhardness tester (Leitz, Wetzlar, Germany), mounted on a multipurpose microscope (Simplex, Opto-Metric Tools Inc, Rockleigh, N.J., USA), and the results were recorded as a percent microhardness change relative to the control group. The microhardness testing correlated the percent of positive or negative enhancement in microhardness between the irradiated and non irradiated (control) root hemi-sections.

### Figure 2: Laser Parameters for Physicochemical Effects

|                           |  |
|---------------------------|--|
| <b>Laser:</b>             | <b>Laser Parameters:</b>   |
| XeCl Pulsed Excimer Laser | Spot Size (SS)= 5.0 mm <sup>2</sup>                              |
| UV (308nm)                | Pulse Duration (PD) = 15ns                                       |
|                           | Pulse Repetition Rate (PRR) = 1, 10 Hz                           |
|                           | Fluence = 0.08 J/cm <sup>2</sup> , 0.24J/cm <sup>2</sup>         |
|                           | Energy Densities = 0.8 J/cm <sup>2</sup> , 2.4 J/cm <sup>2</sup> |

The excimer laser used in our experiments was a short pulse XeCl excimer laser (Lumonics HyperEX-400, Kanata, Ontario, Canada). It emitted 308nm pulses, 15 nanosecond (ns) in duration. The laser output spot size is 36mm by 10mm. After passing through an adjustable iris, the transmitted portion of the pulses was attenuated and focused to achieve the desired energy and spot size on the ablated surface. Maximum energy at the laser's output was 150 milliJoule (mJ).

Following irradiation, each dentin slice was dried for SEM by immersion in increasing concentrations of ETOH (30-100% by volume) and mounted on a stub using colloidal silver liquid (Ted Pella, Inc. Redding, CA.) with the laser treated areas pointing upward, and then gold coated on a PAC-1 Pelco advanced coater 9500 (Ted Pella, Inc. Redding, CA.). Electron micrographs were taken on a Philips 515 (Mohawk, NJ.) scanning electron microscope. Scanning electron microscopy (SEM) was performed to qualitatively compare the extent of microstructural damage due to varying energy and repetition rates.

### 3. Results / Discussion

#### 3.1. Thermal Characteristics

Our thermal measurements show a relatively small range in average temperature gains despite increasing energy per pulse and PRR. Average temperatures gains at the point of impact ranged from 35 - 60 °C, depending on the PRR and energy output. We observed that with this laser, the mechanism of ablation does not appear to be caused by pyrolysis, but rather the destruction of tissue due to the direct photo-decomposition of dentin and subsequent violent expulsion.

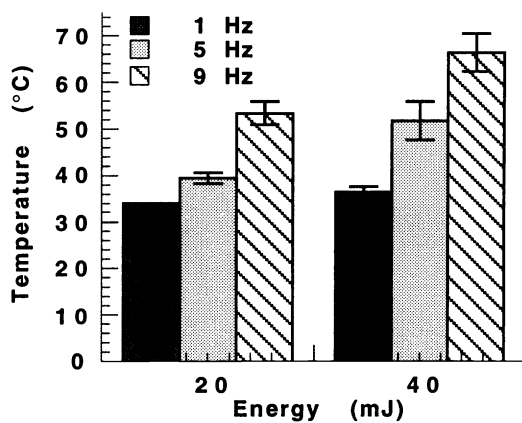


Figure 3: "Hotspot" (HS) temperature as a function of energy output for the 15 ns XeCl laser on fresh dentin. The average temperature gain is relatively small even at 40mJ and 9Hz.

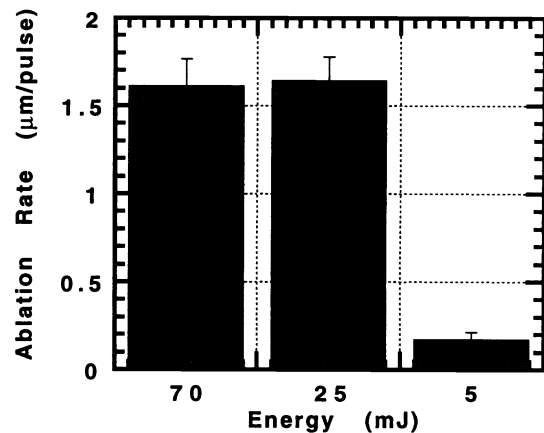


Figure 4: The ablation rate (AR) as a function of energy output for the 15ns XeCl laser on fresh dentin. The AR was measured as the ratio of the depth of penetration in dentin after 100 pulses.

The hot spot (HS) temperatures were observed to increase linearly with PRR but were not as dramatically affected by increases in pulse energy. This is evident in Figure 3, where nearly a 2-fold increase in temperature occurs going from 1 Hz to 9 Hz. Interestingly, at 1Hz PRR, where some rather dramatic changes in microhardness occur, there are very few observed changes in surface temperatures. An important factor reducing tooth heating may be the presence of water retained in the tooth slice during irradiation. In our study, the slices were not allowed to dry out in the air before the onset of irradiation in order to maintain the moisture of the teeth. However, this only partly explains the small variation in temperatures recorded. At all parameters tested, HS temperatures which can be resolved by the 33ms time resolution of our camera, are well below the threshold for carbonization or observed tissue modification. In a separate set of experiments (10) we have determined that for the parameters used in this study, thermal penetration depth even at as high a PRR as 35Hz was below 1.5 mm and no thermal perturbation were registered at the canal.

#### 3.2. Ablation Characteristics

Freshly sliced dentin shows a steep increase in ablation rate that plateaus near 25 mJ/pulse. After 100 pulses at 20 mJ, the ablation rate measured by depth of penetration appears to reach a maximum near 150 microns when ablation depth is determined interferometrically. Any further increases in energy does not produce a deeper crater. Interferometric light microscopy shows that increasing fluence creates larger craters in terms of cross-sectional area. Hence, the amount of mass expelled from the crater and the volume of the crater continue to increase with increasing energy (Figure 4, above).



Figure 5: Glazed tubules and spherical microparticles (plugs) are observed on the surface of the ablation crater.

Scanning electron microscopy (Figure 5) reveals the typical surface characteristics of XeCl ablation. Superficial morphological ablation marks such as the existence of spherical tubule “plugs” and carbonized debris in the crater are observed. However, the “cold ablation” character of this laser is portrayed by the low amount of carbonization and charred residue. This may also be a result of the water content inside the tooth. The presence of water may be minimizing the laser trauma (in terms of carbonization and cracking) by reducing the average temperature of the HS.

### 3.3. Physicochemical Effects

The results in Figure 6 (next page) indicate that at 10 Hz the following microhardness trend is observed. The initial ten pulses at 80 mJ/pulse, yield an 11% increase in microhardness. Thirty pulses result in a relatively large drop (-13%) in microhardness. Ten pulses at higher energy again yield about an 11% increase. Dentin softening depends more on the number of pulses than on the energy per pulse. It thus seems reasonable to conclude that for these low test fluences the initial pulses increase microhardness, while subsequent pulses reverse the effect. We can speculate that this is because the initial laser pulses compromise organic collagen in the dentin while the cumulative effect of the subsequent pulses (perhaps of mechanical origin) compromises some of the mineral component. This “first pulses” effect is then confirmed by the fact that microhardness is again increased following ablation by the first ten 240 mJ pulses.

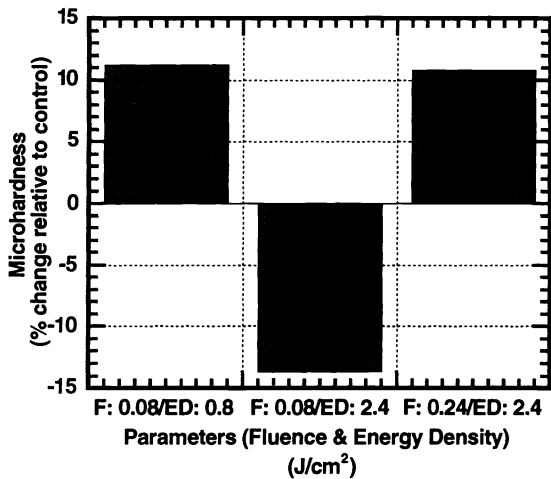


Figure 6: Percent change in microhardness at high PRR.

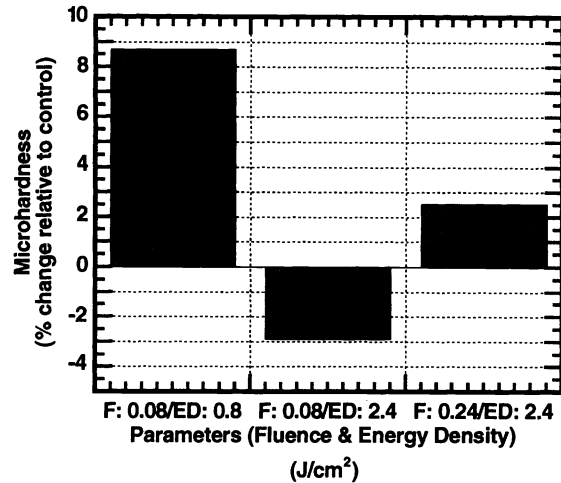


Figure 7: Percent change in microhardness at low PRR

A microhardness test at 1 Hz and 80 mJ (Figure 7) shows that initially there is a significant 8% increase. Again, these changes in microhardness are a consequence of the interaction with the first ten pulses. Subsequent interaction, however, (up to 30) appear to reduce microhardness. Ten pulses yielded a small increase in microhardness. The first ten 240 mJ pulses, again, increased microhardness. It is interesting, however, that these increases are lower for higher pulse energies. This may be due to the fact that increased fluence begins to compromise mineral component integrity as well.

Our overall interpretation on the effect of PRR on microhardness is as follows. Higher PRR generate more steady state (slow) heating which is removed principally by conduction. This smaller amount of heat must be dispensed through diffusion to deeper layers of the dentin. This heat is sufficient to raise the temperature to levels which break down the organic component of the dentin but not its mineral component. Consequently, tissue microhardness is enhanced. Thus, the higher PRR values that we tested at 10 Hz result in enhanced microhardness in comparison to 1 Hz.

Furthermore, the explanation for the observed reduction in microhardness following irradiation by a larger number of pulses may be traced to the increase in crater depth. It is possible that increases in crater depth results in further confinement of ejected debris and gases, thus increasing mechanical stresses on the crater bottom and lateral pressure on the walls. These, in turn, would result in increased microfracturing, and damage to mineral components.

Our SEM photos show that at high PRR and low number of pulses, the largest increases in microhardness occur but great structural damage accompanies the changes (Figure 9). This trend is also seen at lower PRR with a smaller increase in microhardness but less structural damage (Figure 10).



Figure 9: Photos taken from SEM show the greatest structural damage in this group, which was irradiated with the largest fluence at high PRR and had the greatest increase in microhardness.

Figure 10: Microhardness increased modestly here. Less structural damage is seen on the surface of the crater.

Figure 11: Microhardness decreased for this group. Very little structural damage is observed.

By contrast, at higher energy densities (more than 10 pulses), microhardness decreases with minimal structural damage (Figure 11). Thus, there is an apparent inverse proportionality between the degree of microhardness enhanced by the laser and the extent of physical damage done by the laser. However, a more appropriate method would need to be developed to determine the structural damage quantitatively. Current methods use the scanning electron microscope (SEM) to reveal the extent of damage caused by each parameter. Surface charring and cracking are more prevalent and easily observed at high PRR. Also, the smear layer is significantly removed from the surface at higher fluence parameters leaving the irradiated dentinal surface relatively smooth and clean.

#### **4. Conclusions**

Ablation of fresh dentin slices with the XeCl laser appear to be a process of involving small temperature increases at the PRR investigated. At the same time our SEM studies showed dentin melting at fluences as small as  $0.3 \text{ J/cm}^2$  and at PRR as slow as 1Hz, has been shown in previous studies by our group to yield significant if superficial dentin melting and resolidification on the surface. We therefore conclude that rapid thermal buildup are quickly dissipated, and the bulk of the tooth is not effected at the parameters studied here. These observations combined with the low PRR makes the 15ns 308nm pulses of this system ideal for surface preparation but poor for hard tissue removal.

Our studies also showed an increase in microhardness with the first few pulses but a reversal of the effect with additional pulses. We hypothesized that the initial pulses are sufficient to remove organic components of the dentin but do not damage the mineral structure. Additional pulses may then compromise mineral component strength thus reducing microhardness. Interestingly, an increase in microhardness is accompanied by great microstructural damage while a decrease in microhardness often results in very little microstructural damage. Further experimentation is required to fully understand this perplexing observation.

#### **5. Acknowledgments**

This work was supported by the following grants ONR N0014-91-C-0134, DOE DE-FG03-91ER61227 and NIH 5P41RR01192. The authors of this paper would like to acknowledge Randy Slates, Belinda Simonian, and Alan Nguyen for their technical support.



## **6. References**

1. Stern RH, Sognaes RF. Laser beam effect on dental hard tissues *J. Dent Res* 1964, 43:873.
2. Willenborg GC. Dental laser applications: emerging to maturity. *Laser Surg Med* 1989; 9:309-313
3. Neev J, Raney D V, Whalen W E, Fujishige J T, Ho P D, McGrann J V, Berns M W. Ablation of hard dental tissues with ArF pulsed Excimer Laser, in *Laser-Tissue Interaction II, Proceedings of the SPIE: Los Angeles 1991*, S. Jacques, editor, vol. 1427, 162-172.
4. Neev J, Liaw L L, Raney D V, Fujishige J T, Ho P D, Berns M W. "Selectivity and efficiency in the ablation of hard Dental tissue with ArF pulsed excimer lasers", *Lasers in Surgery and Medicine*, No11, December 1991, 499-510.
5. Wigdor H, Abt E, Ashrafi S, Walsh JT. The effect of lasers on hard dental tissues. *J Am Dent Assoc* 1993, 124:65-70
6. Pick RM. Using laser in clinical dental practice. *J Am Dent Assoc* 1993, 124:37-47
7. White JM, Neev J, Goodis H, and Berns MW, Surface temperature and penetration depth of Nd:YAG laser on Enamel and Dentin. *SPIE, Vol 1643 Laser Surgery: 423-436*, 1992.
8. White J.M., Goodis H.E., Kudler J.J., Eakle W.S., Neev J. Histologic and SEM evaluation of Caries removal and restoration in enamel and dentin using a pulsed fiber optic delivered Nd:YAG laser. *SPIE 94 ( In Press)*
9. White J.M., Goodis H.E., Hennings D., Ho W., Hipona C.T. Dentin ablation rate using Nd:YAG and Er:YAG lasers. *J Dent Res* 1994; 73:318 Abstract #1733
10. Neev J, Stabholz A, Liaw L L, Torabinejad M, Fujishige J T, Ho P H, Berns M W. "Scanning Electron Microscopy and Thermal characteristics of Dentin ablated by a short-pulse XeCl Laser", *Lasers in Surgery and Medicine Vol 13, No 3:353-361*, 1993.
11. Frentzen M, Koort HJ, Nolden R. [Root canal preparation using Excimer lasers]. *Deutsche Zahnärztliche Zeitschrift*, 1991 Apr, 46(4):288-9. Language: German
12. Pini R., Salimbeni R., Vannini M., Barone R., and Clauser C. Laser dentistry: A new application of excimer laser in root canal therapy. *Laser Surg Med* 1989; 9:352-357.
13. Neev J, Raney D V, Whalen W E, Fujishige J T, Ho P D, McGrann J V, and Berns M W, "Dentin ablation with two excimer lasers: A comparative study of physical characteristics", *Lasers in the Life Sciences*, 4(3), 1992, pp1-25.
14. Nelson DG; Coote GE; Shariati M; Featherstone JD. High resolution fluoride profiles of artificial in vitro lesions treated with fluoride dentifrices and mouth rinses during pH cycling conditions. *Caries Research*, 1992, 26(4):254-62.
15. Meyerowitz C, Featherstone JD, Billings RJ, Eisenberg AD, Fu J, Shariati M, Zero DT. Use of an intra-oral model to evaluate 0.05% sodium fluoride mouthrinse in radiation-induced hyposalivation. *Journal of Dental Research*, 1991 May, 70(5):894-8.
16. Featherstone JD, Zero DT. An in situ model for simultaneous assessment of inhibition of demineralization and enhancement of remineralization. *Journal of Dental Research*, 1992 Apr, 71 Spec No: 804-10.
17. Burkes EJ Jr, Hoke J, Gomes E, Wolbarsht M. Wet versus dry enamel ablation by Er:YAG laser. *Journal of Prosthetic Dentistry*, 1992 Jun, 67(6):847-51.